Inorg. Chem. **2008**, *47*, 11197−11201

An Approach to the Synthesis of Polyoxometalate Encapsulating Different Kinds of Oxoanions as Heteroions: Bisphosphitopyrophosphatotriacontamolybdate $[(HPO_3)_2(P_2O_7)Mo_{30}O_{90}]^{8-}$

Sayuri Maeda,[†] Takuya Goto,[†] Masayo Takamoto,[†] Kazuo Eda,*[,†] Sadayuki Himeno,[†] Hiroki Takahashi,[‡] and Toshitaka Hori[‡]

Department of Chemistry, Graduate School of Science, Kobe University, Kobe 657-8501, and Graduate School of Human and Environmental Studies, Kyoto University, Kyoto 606-8501

Received August 7, 2008

A yellow $[(HPO_3)_2(P_2O_7)Mo_{30}O_{90}]^{8-}$ anion was prepared as a tetrapropylammonium (Pr_4N^+) salt from a 50 mM Mo^{VI}−2 mM $P_2O_7^{4-}$−4 mM HPO_3^{2-}−0.95 M HCl−60% (v/v) CH_3CN system at ambient temperature. The $(Pr_4N)_8[(HPO_3)_2(P_2O_7)Mo_{30}O_{90}]$ salt crystallized in the orthorhombic space group P_{nma} (No. 62), with $a = 30.827(2)$ Å, $b = 22.8060(15)$ Å, $c = 30.928(2)$ Å, $V = 21743(3)$ Å^3, and $Z = 4$. The structure contained a $(P_2O_7)Mo_{12}O_{42}$ fragment derived from the removal of each corner-shared Mo_3O_{13} unit in a polar position from a $[(P_2O_7)Mo_{18}O_{54}]^{4-}$ structure, and each side of the $(P_2O_7)Mo_{12}O_{42}$ fragment was capped by a B-type $(HPO_3)Mo_9O_{24}$ unit. The $[(HPO_3)_2(P_2O_7)Mo_{30}O_{90}]^{8-}$ anion was characterized by voltammetry and IR, UV−vis, and ^{31}P NMR spectroscopy. Unlike the Keggin and Dawson anions and the parent $[(P_2O_7)Mo_{18}O_{54}]^{4-}$ anion, the $[(HPO_3)_2(P_2O_7)Mo_{30}O_{90}]^{8-}$ anion exhibited two-electron redox waves in CH_3CN with and without acid.

Introduction

So far, the major part of the polyoxometalate (POM) chemistry concerns the study of Keggin and Dawson complexes incorporating XO_4-type heteroions and of their mixed-addenda derivatives in which Mo or W atoms are partially substituted by other metal atoms. There has been a growing interest in the structures and chemical properties of POMs. The structure of POM is mainly dependent on the stereochemistry of the central oxoanion being capable of acting as a heteroion. Therefore, one possible approach is to prepare POMs incorporating mixed heteroatoms as central heteroions, and several POMs incorporating H and X have been reported; $[H_4PW_{18}O_{62}]^{7-}$ and $[H_nXW_{18}O_{60}]^{m-}$ ($n = 2$, 3; X = As^{III}, Sb^{III}, Bi^{III}; $m = 7$, 6).[1]

Recently, POMs based on pyrophosphate ($P_2O_7^{4-}$) received increasing attention, because $P_2O_7^{4-}$ can utilize six oxygen atoms to bind POM structures, and several POMs with new structural types have already been prepared.[2] As far as pyrophosphatomolybdates are concerned, we prepared $[(P_2O_7)Mo_{18}O_{54}]^{4-}$ from an acidified 50 mM Mo^{VI}−5.0 mM $P_2O_7^{4-}$−60% (v/v) CH_3CN system.[3] Unlike the Dawson-type $[P_2Mo_{18}O_{62}]^{6-}$ structure based on two A-type PMo_9 units, the $[(P_2O_7)Mo_{18}O_{54}]^{4-}$ structure contains two B-type PMo_9 units.[4] Although $[(P_2O_7)Mo_{18}O_{54}]^{4-}$ is kinetically stable in the Mo^{VI}−$P_2O_7^{4-}$−60% (v/v) CH_3CN system, it becomes unstable at lower CH_3CN concentrations or $[Mo^{VI}]/[P_2O_7^{4-}]$ ratios, being transformed, via $[H_6(P_2O_7)Mo_{15}O_{48}]^{4-}$, into $[H_{12}(P_2O_7)Mo_{12}O_{42}]^{4-}$.[5,6] According to Kortz, the $(C_4H_9)_4N^+$ (Bu_4N^+) salt of the lacunary $[H_6(P_2O_7)Mo_{15}O_{48}]^{4-}$ ion is

* To whom correspondence should be addressed. E-mail: eda@kobe-u.ac.jp.
† Kobe University.
‡ Kyoto University.

(1) (a) Jeannin, Y.; Martin-Frere, J. *Inorg. Chem.* **1979**, *18*, 3010. (b) Ozawa, Y.; Sasaki, Y. *Chem. Lett.* **1987**, 923. (c) Contant, R.; Piro-Sellem, S.; Canny, J.; Thouvenot, R. C. R. *Acad. Sci. Paris, Ser. IIc* **2000**, *3*, 157. (d) Mbomekalle, I.-M.; Keita, B.; Lu, Y. W.; Nadjo, L.; Contant, R.; Belai, N.; Pope, M. T. *Eur. J. Inorg. Chem.* **2004**, 276. (e) Krebs, B.; Klein, R. In *Polyoxometalates: From Platonic Solids to Anti-Retroviral Activity*; Pope, M. T.; Müller, A., Ed.; Kluwer Academic Publishers: Dordrecht, 1994; p 41.

(2) (a) Kortz, U.; Jameson, G. B.; Pope, M. T. *J. Am. Chem. Soc.* **1994**, *116*, 2659. (b) Kortz, U. *Inorg. Chem.* **2000**, *39*, 625. (c) du Peloux, C.; Mialane, P.; Dolbecq, A.; Marrot, J.; Sécheresse, F. *Angew. Chem., Int. Ed.* **2002**, *41*, 2808. (d) Himeno, S.; Katsuta, T.; Takamoto, M.; Hashimoto, M. *Bull. Chem. Soc. Jpn.* **2006**, *79*, 100.

(3) Himeno, S.; Saito, A.; Hori, T. *Bull. Chem. Soc. Jpn.* **1990**, *63*, 1602.

(4) Kortz, U.; Pope, M. T. *Inorg. Chem.* **1994**, *33*, 5643.

(5) Himeno, S.; Kubo, T.; Saito, A.; Hori, T. *Inorg. Chim. Acta* **1995**, *236*, 167.

(6) Himeno, S.; Ueda, T.; Shiomi, M.; Hori, T. *Inorg. Chim. Acta* **1997**, *262*, 219.

10.1021/ic801499y CCC: $40.75
Published on Web 10/18/2008

actually a dimeric species with the formula of $(Bu_4N)_2H_9[(P_2O_7)_2Mo_{30}O_{90}]\cdot[PMo_{12}O_{40}]$; the dimeric anion is always cocrystallized with the Keggin-type $[PMo_{12}O_{40}]^{3-}$ anion.[7]

Besides, the structure and chemical properties of phosphitomolybdates still remain to be elucidated, because HPO_3^{2-} possesses only three oxygen atoms available for binding, and the resulting POM structure must adapt an H atom occupying a tetrahedral vertex. We found that Mo^{VI}can react directly with HPO_3^{2-} to form $[H_6(HPO_3)_2Mo_{15}O_{48}]^{4-}$ in an acidified 50 mM Mo^{VI}−5.0 mM HPO_3^{2-}−60% (v/v) CH_3CN system and its spontaneous conversion into $[H_{12}(HPO_3)_2Mo_{12}O_{42}]^{4-}$ at lower $[Mo^{VI}]/[HPO_3^{2-}]$ ratios.[8]

Thus, remarkable progress has been made with the use of CH_3CN in the preparation procedure of POMs. Since the $[(P_2O_7)Mo_{18}O_{54}]^{4-}$ and $[H_6(HPO_3)_2Mo_{15}O_{48}]^{4-}$ anions have common properties of being spontaneously converted into other species with lower Mo/P ratios in such CH_3CN−water mixed solvents, we extend these findings to devise new synthetic procedures for POMs encapsulating both $P_2O_7^{4-}$ and HPO_3^{2-} ions. The synthesis of polyanions encapsulating simultaneously different types of oxoanions remains a challenging area in the POM chemistry.

In the present study, we succeeded in preparing a previously unknown $[(HPO_3)_2(P_2O_7)Mo_{30}O_{90}]^{8-}$ complex from an acidified Mo^{VI}−60% (v/v) CH_3CN system containing $P_2O_7^{4-}$ and HPO_3^{2-}. In contrast to the parent $[(P_2O_7)Mo_{18}O_{54}]^{4-}$ and $[H_6(HPO_3)_2Mo_{15}O_{48}]^{4-}$ anions, $[(HPO_3)_2(P_2O_7)Mo_{30}O_{90}]^{8-}$ was resistant toward decomposition in such aqueous−CH_3CN media. Here, we report the synthesis, structure, and characterization of the new heteropolyanion.

Results and Discussion

Syntheses. $(Pr_4N)_8[(HPO_3)_2(P_2O_7)Mo_{30}O_{90}]$. The synthetic procedure involves the formation reactions of $[(P_2O_7)Mo_{18}O_{54}]^{4-}$ and $[H_6(HPO_3)_2Mo_{15}O_{48}]^{4-}$ and their subsequent conversion reactions, leading to $[(HPO_3)_2(P_2O_7)Mo_{30}O_{90}]^{8-}$. To a solution of 6.0 g of $Na_2MoO_4\cdot2H_2O$ (25 mmol), 0.45 g of $Na_4P_2O_7\cdot10H_2O$ (1.0 mmol), and 0.16 g of H_3PO_3 (2.0 mmol) in 150 mL of water was added dropwise 47.5 mL of 10 M HCl with vigorous stirring, followed by the addition of 300 mL of CH_3CN. After the yellow solution was stirred with a magnetic stirrer for 2 h at ambient temperature, 15 g of Pr_4NBr was added to yield a yellow salt, which was collected by vacuum filtration, washed with water and hot acetone, and air-dried. Yield, 0.95 g (19% based on Mo). The yellow salt was purified by recrystallization from a 60% (v/v) CH_3CN−water solution, washed with acetone to remove any remaining traces of $(Pr_4N)_3[PMo_{12}O_{40}]$, and recrystallized again from CH_3CN. Crystallization of the Pr_4N^+ salt in CH_3CN gave suitable-quality crystals for an X-ray structure determination. Found: C, 18.7; H, 3.6; N, 1.9; Mo, 47.2; P, 2.1%. Calcd for $(Pr_4N)_8[(HPO_3)_2(P_2O_7)Mo_{30}O_{90}]$: C, 18.8; H, 3.7; N, 1.8; Mo, 46.9; P, 2.0%. IR (KBr, cm^{-1}): 1173, 1121, 1068, 994, 947, 867, 788, 521.

It should be added that crystallization of the Bu_4N^+ salt always gives single crystals of $[(HPO_3)_2(P_2O_7)Mo_{30}O_{90}]^{8-}$ cocrystallized with the Keggin-type $[PMo_{12}O_{40}]^{3-}$ anion. Found: C, 23.1; H, 4.2; N, 1.7%. Calcd for $(Bu_4N)_8[(HPO_3)_2(P_2O_7)Mo_{30}O_{90}]\cdot1.5(Bu_4N)_3[PMo_{12}O_{40}]$: C, 22.8; H, 4.4; N, 1.7%. IR (KBr, cm^{-1}): 1173, 1121, 1064, 994, 953, 879, 792, 521. However, only six Bu_4N^+ cations were located crystallographically, owing to disorder. Similar cocrystallization and disorder behaviors were also reported by Kortz for $(Bu_4N)_2H_9[(P_2O_7)_2Mo_{30}O_{90}]\cdot[PMo_{12}O_{40}]$.[7]

In order to analyze ^{31}P NMR spectra in acidified Mo^{VI}−$P_2O_7^{4-}$−HPO_3^{2-}−60% (v/v) CH_3CN media, $(Bu_4N)_4[(P_2O_7)Mo_{18}O_{54}]$ (−24.0 ppm), $(Pr_4N)_3H[H_{12}(P_2O_7)Mo_{12}O_{42}]$ (−25.4 ppm), and $(Bu_4N)_4[H_6(HPO_3)_2Mo_{15}O_{48}]$ (5.6 ppm (doublet, J_{PH} = 682 Hz), 17.5 ppm (doublet, J_{PH} = 742 Hz)) were prepared according to our previous procedures,[3,6,8] being used as reference compounds. The numerals in parentheses denote their ^{31}P NMR chemical shift values in a 60% (v/v) CH_3CN−0.50 M $HClO_4$ system.

Crystal Structure Determination. Crystallization of $(Pr_4N)_8[(HPO_3)_2(P_2O_7)Mo_{30}O_{90}]$ in CH_3CN gave suitable-quality crystals for an X-ray structure determination. When exposed to air, however, the crystals became opaque owing to a loss of the solvent of crystallization. Therefore, crystals coated with epoxy resin were subjected to an X-ray diffraction measurement.

Most of the diffractions at $2\theta > 40°$ were remarkably weak, probably because the crystal might contain diffuse solvent, and positional and orientational disorders in its structure. To attempt a more accurate determination, more than twenty crystals were measured,[9] and we reached a reasonable structural determination (Table 1).[10] As shown in Figure 1a, the $[(HPO_3)_2(P_2O_7)Mo_{30}O_{90}]^{8-}$ anion encapsulated two phosphites and one pyrophosphate in it. The unit cell was composed of 4 $[(HPO_3)_2(P_2O_7)Mo_{30}O_{90}]^{8-}$ anions and 32 Pr_4N^+ cations (eight Pr_4N^+s per anion, and five kinds, three whole and two half, of Pr_4N^+ cations as asymmetic unit). Although the anion possesses no center of symmetry, the respective phosphorus sites of two phosphites and of a pyrophosphate are geometrically almost equivalent (symmetric against a virtual mirror shown in Figure 1a). These

(7) Kortz, U. *Inorg. Chem.* **2000**, *39*, 623.
(8) Ueda, T.; Sano, K.; Himeno, S.; Hori, T. *Bull. Chem. Soc. Jpn.* **1997**, *70*, 1093.

(9) In the present structural determination, many atoms could not be refined anisotropically. There were some very large, anisotropic displacement parameters (for example, Mo16 and O16). Such very large anisotropic displacement parameters and not-well-lowered R indexes ($R_1 = 0.11$ and $wR_2 = 0.29$) often are evidence of disorder and/or twinning. We tested some twinning (merohedral and pseudomerohedral twinning such as a (100) twin in $P2_1/n$) and further disorder (for example, ones concerning Mo16 and O16, see Figure S1, Supporting Information for atom-labeling) models, but no improvements were obtained in the structure refinements. In the final difference map, the deepest hole was −3.44 e $Å^{-3}$ near the Mo16 position and the highest peak 5.19 e $Å^{-3}$ near the P3 position. The highest peak was tested as the P atom, which gave an atomic occupancy of almost zero. It must be added that measurements with the use of Cu $K\alpha$ radiation (1.5418 Å) gave no improvements in the structure refinements.

(10) The present structural solution showed that there still was 4400 $Å^3$ of void volume in the unit cell, indicating the presence of a lot of diffuse solvent (acetonitrile molecules). We estimated the existence of ca. 40−50 acetonitrile molecules in the solvent-accessible void, since one acetonitrile molecule was calculated to occupy ca. 100 $Å^3$. These acetonitrile molecules were easily released from the crystal, because the elemental analysis data were in good agreement with those for $(Pr_4N)_8[(HPO_3)_2(P_2O_7)Mo_{30}O_{90}]$ (without acetonitrile).

Table 1. Crystal Data and Structure Refinement for $(Pr_4N)_8[(HPO_3)_2(P_2O_7)Mo_{30}O_{90}]$

crystal system	orthorhombic	index range	h: −39 to 32
space group	*Pnma*		k: −28 to 28
a/Å	30.827(2)		l: −38 to 36
b/Å	22.8060(15)	reflection collected	101747
c/Å	30.928(2)	reflection unique	22331
cell volume/Å^3	21743(3)	R_{int}	0.0847
Z	4	reflection ($I > 2\sigma(I)$)	12094
temperature/K	193	number of parameters	1085
crystal color	yellow	$R_1(F)$ ($I > 2\sigma$ (I))	0.1147
crystal size/mm	0.30 × 0.20 × 0.17	$wR_2(F^2)$ for all reflection	0.2921
μ (Mo Kα)/mm^{-1}	1.773	goodness-of-fit	1.124
F(000)	12008	max shift/esd	0.001
theta range/°	3.19−26.89	ρ_{max}/e Å^{-3}	5.194
		ρ_{min}/e Å^{-3}	−3.438

structural and compositional features of $[(HPO_3)_2(P_2O_7)Mo_{30}O_{90}]^{8-}$ are compatible with the ^{31}P NMR results, as described below. The $[(HPO_3)_2(P_2O_7)Mo_{30}O_{90}]^{8-}$ anion possesses the structure closely related to a cigar-shaped $[(P_2O_7)_2Mo_{30}O_{90}]^{8-}$ anion (Figure 1b).[7]

The Pr_4N^+ cations were hydrogen-bonded and/or attracted by Coulomb force to the surface of $[(HPO_3)_2(P_2O_7)Mo_{30}O_{90}]^{8-}$ (Table S1, Supporting Information). Three (Pr_4N^+2,3,4) of five kinds of Pr_4N^+ cations occupied general positions of the crystal, while the remaining two (Pr_4N^+1,5) were on the mirror plane where $[(HPO_3)_2(P_2O_7)Mo_{30}O_{90}]^{8-}$ was also located (Figure S1, Supporting Information). The conformation of Pr_4N^+1 was symmetric against the mirror (atomic distance $D_{O14-C9} = D_{O14^m-C9^m} = 3.38$ Å in Figure S1, Supporting Information), but that of Pr_4N^+5 was asymmetric ($D_{O5-C57} \neq D_{O5^m-C51}$ and $D_{O8-C48} \neq D_{O8^m-C54}$ in Figure S1, Supporting Information). Therefore, Pr_4N^+5s having original and mirror-image conformations should be randomly present in equivalent numbers in the crystal. The original and mirror-image conformations exhibit equivalent interactions with surrounding molybdo-anions and Pr_4N^+ cations, leading to an orientational disorder.

^{31}P NMR Spectra. Both $(Pr_4N)_8[(HPO_3)_2(P_2O_7)Mo_{30}O_{90}]$ and $(Bu_4N)_8[(HPO_3)_2(P_2O_7)Mo_{30}O_{90}]\cdot 1.5(Bu_4N)_3[PMo_{12}O_{40}]$ are soluble in CH_3CN to give yellow solutions. The proton-decoupled ^{31}P NMR spectrum shows two singlet peaks with equal integrated intensities at 16.3 (doublet without proton-decoupling, $J_{PH} = 733$ Hz) and −24.4 ppm (Figure 2), whereas the cigar-shaped $[(P_2O_7)_2Mo_{30}O_{90}]^{8-}$ anion shows ^{31}P NMR lines at −21.7 (doublet) and −23.6 (doublet) ppm in CD_3CN ($^2J_{PP} = 36.0$ Hz).[7] The ^{31}P NMR result is consistent with the structure of $[(HPO_3)_2(P_2O_7)Mo_{30}O_{90}]^{8-}$, indicating that the solid-state structure is retained in CH_3CN. The −2.4 ppm line in Figure 2b is due to $[PMo_{12}O_{40}]^{3-}$.

In the following, the $(Pr_4N)_8[(HPO_3)_2(P_2O_7)Mo_{30}O_{90}]$ salt was used to study the chemical properties of $[(HPO_3)_2(P_2O_7)Mo_{30}O_{90}]^{8-}$.

UV−vis Spectra. The $[(HPO_3)_2(P_2O_7)Mo_{30}O_{90}]^{8-}$ anion exhibited a UV−vis spectrum like a shoulder around 310 nm; the molar absorption coefficient (ε_{max}) was found to be 5.47×10^4 mol^{-1}dm^{3}cm^{-1} at this wavelength (Figure S2, Supporting Information). The solution obeyed Beer's law in the spectral region studied. However, the UV−vis spectrum was affected by the presence of H^+. As shown in Figure S2, Supporting Information, the absorbance values at wavelengths of 300−500 nm increased with the H^+ concentration up to 6.0×10^{-5} M. Since no further spectral change is observed above this concentration, this behavior can be accounted for in terms of the formation of diprotonated form, $H_2[(HPO_3)_2(P_2O_7)Mo_{30}O_{90}]^{6-}$, which is kinetically stable in CH_3CN, as judged by no spectral change with time.

Electrochemistry. Keggin and Dawson anions have been the subject of extensive voltammetric studies.[11] It is well-known that both Keggin and Dawson anions undergo successive one-electron reductions in neutral media where no protonation accompanies electrochemical reduction. The presence of H^+ caused the one-electron waves to merge into two-electron waves, owing to the protonation of the reduced form at the electrode surface. Besides, the presence of Li^+ or Na^+ instead of H^+ also produced two-electron waves.[11k]

Figure 3a shows a cyclic voltammogram of 0.50 mM $[(HPO_3)_2(P_2O_7)Mo_{30}O_{90}]^{8-}$ in CH_3CN containing 0.10 M $(C_5H_{11})_4NClO_4$. We found a redox wave with a midpoint potential (E_{mid}) of −0.33 V, followed by a reduction wave at −1.02 V, where $E_{mid} = (E_{pc} - E_{pa})/2$; E_{pc} and E_{pa} are the cathodic and anodic peak-potentials, respectively. Both waves are diffusion-controlled. According to the coulometric and normal pulse voltammetric measurements, both reduction waves corresponded to two-electron transfers. The separation of the E_{pc} and E_{pa} value for the first wave was 34 mV, indicating the reversible nature of the two-electron wave. Controlled potential electrolysis at the first reduction wave produced a mixed-valence blue species, which was reverted to the original yellow $[(HPO_3)_2(P_2O_7)Mo_{30}O_{90}]^{8-}$ anion by the reoxidation at +0.10 V. On the other hand, the second reduction wave at −1.02 V did not exhibit a corresponding oxidation wave on the reverse anodic scan, indicating that the two-electron reduction species accepts further electrons with the subsequent decomposition.

$$[(HPO_3)_2(P_2O_7)Mo_{30}O_{90}]^{8-} + 2e^- = [(HPO_3)_2(P_2O_7)Mo_2^VMo_{28}O_{90}]^{10-}$$

$$[(HPO_3)_2(P_2O_7)Mo_2^VMo_{28}O_{90}]^{10-} + 2e^- \rightarrow \text{decomposition}$$

The voltammetric behavior was very sensitive to the presence of traces of H^+. In the presence of 1.0 mM H^+ (Figure 3b), an ill-defined wave was obtained at a potential more positive than the first two-electron wave, owing to the protonation of the oxidized form (Figure S2c, Supporting Information). With further increase of the H^+ concentration, a new wave grew at slightly positive potentials, indicating

(11) (a) Maeda, K.; Himeno, S.; Osakai, T.; Saito, A.; Hori, T. *J. Electroanal. Chem.* **1994**, *364*, 149. (b) Sadakane, M.; Steckhan, E. *Chem. Rev.* **1998**, *98*, 219. (c) Way, D. M.; Cooper, J. B.; Sadek, M.; Vu, T.; Mahon, P. J.; Bond, A. M.; Brownlee, R. T. C.; Wedd, A. G. *Inorg. Chem.* **1997**, *36*, 4227. (d) Prenzler, P. D.; Boskovic, C.; Bond, A. M.; Wedd, A. G. *Anal. Chem.* **1999**, *71*, 3650. (e) Way, D. M.; Bond, A. M.; Wedd, A. G. *Inorg. Chem.* **1997**, *36*, 2826. (f) Bond, A. M.; Vu, T.; Wedd, A. G. *J. Electroanal. Chem.* **2000**, *494*, 96. (g) Himeno, S.; Takamoto, M.; Santo, R.; Ichimura, A. *Bull. Chem. Soc. Jpn.* **2005**, *78*, 95. (h) López, X.; Fernández, J. A.; Poblet, J. M. *Dalton Trans.* **2006**, 1162. (i) Richardt, P. J. S.; Gable, R. W.; Bond, A. M.; Wedd, A. G. *Inorg. Chem.* **2001**, *40*, 703. (j) Zhang, J.; Bond, A. M.; Richardt, P. J. S.; Wedd, A. G. *Inorg. Chem.* **2004**, *43*, 8263. (k) Himeno, S.; Takamoto, M.; Ueda, T. *J. Electroanal. Chem.* **2000**, *485*, 49.

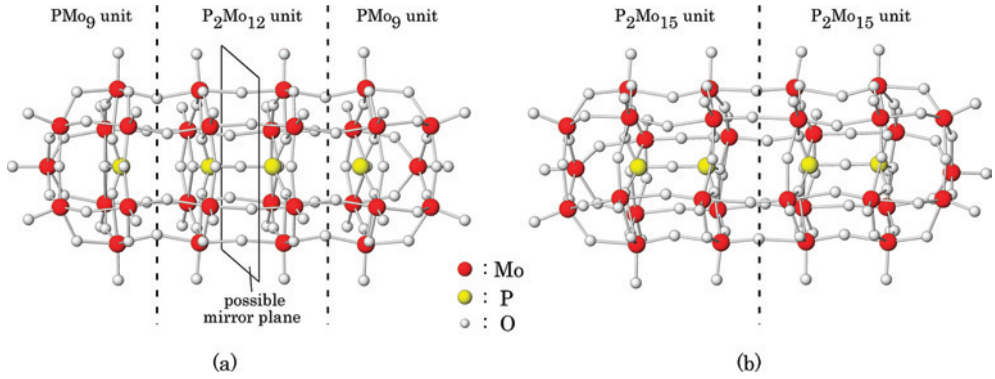

Figure 1. Structures of (a) $[(HPO_3)_2(P_2O_7)Mo_{30}O_{90}]^{8-}$ and (b) $[(P_2O_7)_2Mo_{30}O_{90}]^{8-}$ (after ref 7). Reprinted with permission from ref 7. Copyright 2000 American Chemical Society.

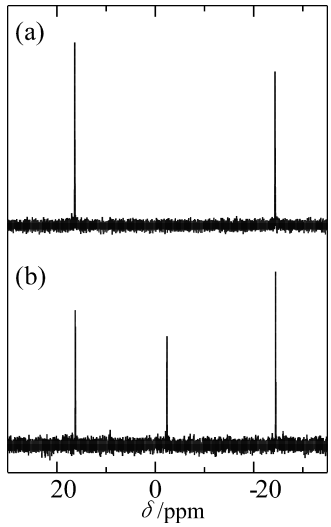

Figure 2. Proton-decoupled ^{31}P NMR spectra of (a) $(Pr_4N)_8[(HPO_3)_2(P_2O_7)Mo_{30}O_{90}]$; (b) $(Bu_4N)_8[(HPO_3)_2(P_2O_7)Mo_{30}O_{90}]\cdot 1.5(Bu_4N)_3[PMo_{12}O_{40}]$ dissolved in CH_3CN. Numerical data are given in the text.

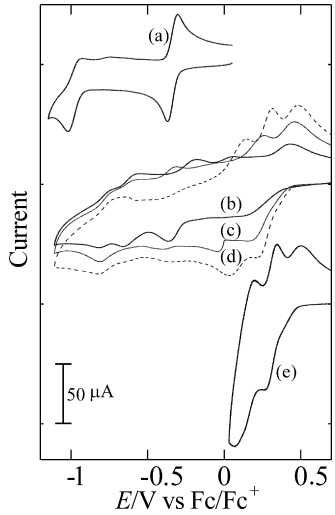

Figure 3. Cyclic voltammograms of 0.50 mM $[(HPO_3)_2(P_2O_7)Mo_{30}O_{90}]^{8-}$ in CH_3CN containing 0.10 M $(C_5H_{11})_4NClO_4$. $[H^+]$/mM: (a) none; (b) 1.0; (c) 3.0; (d) 5.0; (e) 10.

that the electrochemical reduction is accompanied by the protonation.[11] Finally, an apparent two-step reduction wave resulted with a current ratio of 2:1 (Figure 3e), succeeded by ill-defined waves. Normal pulse voltammetric measurements showed that the first and second waves corresponded

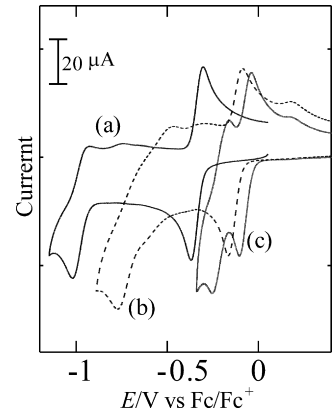

Figure 4. Cyclic voltammograms of 0.50 mM $[(HPO_3)_2(P_2O_7)Mo_{30}O_{90}]^{8-}$ in CH_3CN containing (a) 0.10 M $(C_5H_{11})_4NClO_4$; (b) 0.090 M $(C_5H_{11})_4NClO_4$ + 0.010 M $LiClO_4$; (c) 0.050 M $(C_5H_{11})_4NClO_4$ + 0.050 M $LiClO_4$.

to four- and two-electron transfers, respectively. The first wave is somewhat distorted, probably owing to multistep charge transfers.[12] Indeed, a logarithmic analysis of the normal pulse voltammogram indicates that the reduction waves are composed of three two-electron transfers, with the first two close together.

On the other hand, entirely different behavior was observed in the presence of Li^+ instead of H^+. Figure 4 shows cyclic voltammograms of 0.50 mM $[(HPO_3)_2(P_2O_7)Mo_{30}O_{90}]^{8-}$ in CH_3CN containing $(C_5H_{11})_4NClO_4 + LiClO_4$, where the ionic strength is kept constant at 0.10. At the Li^+ concentration of 0.050 M (Figure 4c), E_{mid} values were found to be -0.07 and -0.21 V. Coulometric analysis confirms that each wave corresponds to a two-electron transfer, indicating that the presence of Li^+ only causes the two-electron waves to shift to more positive potentials. Because the UV−vis spectrum was unchanged by the presence of Li^+, this behavior can be accounted for in terms of the association of the reduced species with Li^+ at the electrode surface.

To our knowledge, $[(HPO_3)_2(P_2O_7)Mo_{30}O_{90}]^{8-}$ is the first example of undergoing two-electron reductions in the absence of H^+. The presence of H^+ or Li^+ produced new two-electron waves at potentials more positive than the original first two-electron wave. These behaviors are in marked contrast to the voltammetric behaviors of Keggin and Dawson complexes.[11]

(12) Polcyn, D. S.; Shain, I. *Anal. Chem.* **1966**, *38*, 370.

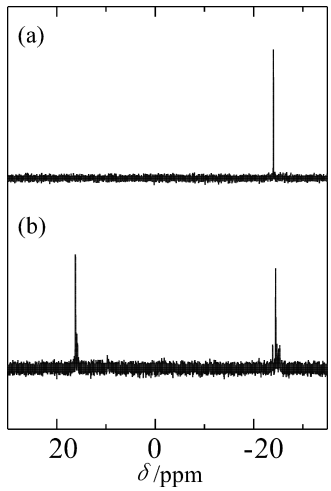

Figure 5. Proton-decoupled ^{31}P NMR spectra for (a) a 100 mM Mo^{VI}−2.5 mM $P_2O_7^{4-}$−0.50 M $HClO_4$−60% (v/v) CH_3CN system; (b) (a) + 5.0 mM HPO_3^{2-}. The ^{31}P NMR spectra were recorded after standing for 24 h at ambient temperature.

Formation Processes of $[(HPO_3)_2(P_2O_7)Mo_{30}O_{90}]^{8-}$. As described above, $[(HPO_3)_2(P_2O_7)Mo_{30}O_{90}]^{8-}$ is prepared by stirring an acidified Mo^{VI}−$P_2O_7^{4-}$−HPO_3^{2-}−60% (v/v) CH_3CN system at ambient temperature. With the aim of clarifying the formation processes of $[(HPO_3)_2(P_2O_7)Mo_{30}O_{90}]^{8-}$, ^{31}P NMR measurements were made for a 100 mM Mo^{VI}−2.5 mM $P_2O_7^{4-}$−0.50 M $HClO_4$−60% (v/v) CH_3CN system. As shown in Figure 5a, we found a ^{31}P NMR line at −24.0 ppm, assigned to $[(P_2O_7)Mo_{18}O_{54}]^{4-}$.[4] The ^{31}P NMR spectrum was unchanged with time, because the presence of free Mo^{VI} can stabilize the $[(P_2O_7)Mo_{18}O_{54}]^{4-}$ structure.[5] With the addition of 5.0 mM HPO_3^{2-} to the solution, the formation of $[(HPO_3)_2(P_2O_7)Mo_{30}O_{90}]^{8-}$ was ascertained by the appearance of two ^{31}P NMR lines of equal integrated intensities at 16.2 (doublet without proton-decoupling, $J_{PH} = 733$ Hz) and −24.5 (singlet) ppm (Figure 5b). It seems likely that $[(P_2O_7)Mo_{18}O_{54}]^{4-}$ becomes kinetically unstable, owing to the consumption of free Mo^{VI} to construct the $[H_6(HPO_3)_2Mo_{15}O_{48}]^{4-}$ structure.[8] This is supported by the fact that $[(HPO_3)_2(P_2O_7)Mo_{30}O_{90}]^{8-}$ is not formed by the addition of 5.0 mM $(Bu_4N)_4[H_6(HPO_3)_2Mo_{15}O_{48}]$ to the 100 mM Mo^{VI}−2.5 mM $P_2O_7^{4-}$−0.50 M $HClO_4$−60% (v/v) CH_3CN system.

In order to study the formation processes more directly, we focused on the reactivity of $[H_{12}(P_2O_7)Mo_{12}O_{42}]^{4-}$ in a 0.50 M $HClO_4$−60% (v/v) CH_3CN system, because the structure of $[(HPO_3)_2(P_2O_7)Mo_{30}O_{90}]^{8-}$ can be viewed as two B-type $(HPO_3)Mo_9O_{24}$ units capping either side of the $(P_2O_7)Mo_{12}O_{42}$ fragment. When a ^{31}P NMR spectrum was recorded 24 h after the addition of 2.4 mM $(Bu_4N)_4[H_6(HPO_3)_2Mo_{15}O_{48}]$ to a 1.2 mM $(Pr_4N)_3H[H_{12}(P_2O_7)Mo_{12}O_{42}]$-0.50 M $HClO_4$−60% (v/v) CH_3CN system, the formation of $[(HPO_3)_2(P_2O_7)Mo_{30}O_{90}]^{8-}$ was ascertained by its characteristic ^{31}P NMR lines. These results indicate that $[H_6(HPO_3)_2Mo_{15}O_{48}]^{4-}$ can function as a source of the $(HPO_3)Mo_9O_{24}$ unit. The coexistence of $[H_{12}(P_2O_7)Mo_{12}O_{42}]^{4-}$ may be essential for the conversion of $[H_6(HPO_3)_2Mo_{15}O_{48}]^{4-}$ to the $(HPO_3)Mo_9O_{24}$ unit, because the conversion product is found to be $[H_{12}(HPO_3)_2Mo_{12}O_{42}]^{4-}$ in an acidified Mo^{VI}−HPO_3^{2-}−60% (v/v) CH_3CN system,[8,13] where $P_2O_7^{4-}$ is absent.

Conclusions

We developed a new route to the preparation of novel POMs encapsulating simultaneously different kinds of oxo-anions. The preparative method involved the formation of a mixture of POMs with different oxo-anions, followed by their subsequent transformation reactions, leading to a novel POM with two different oxo-anions.

In the present paper, $[(P_2O_7)Mo_{18}O_{54}]^{4-}$ and $[H_6(HPO_3)_2Mo_{15}O_{48}]^{4-}$ was formed in the Mo^{VI}−$P_2O_7^{4-}$−HPO_3^{2-}−60% (v/v) CH_3CN system, being spontaneously converted into a novel POM encapsulating $P_2O_7^{4-}$ and HPO_3^{2-}, $[(HPO_3)_2(P_2O_7)Mo_{30}O_{90}]^{8-}$. Thus, the formation reaction could be regarded as the replacement of the corner-shared Mo_3O_6 units by the $(HPO_3)Mo_9O_{24}$ units. The $[(HPO_3)_2(P_2O_7)Mo_{30}O_{90}]^{8-}$ structure was closely related to a cigar-shaped $[(P_2O_7)_2Mo_{30}O_{90}]^{8-}$ structure reported by Kortz.[7] The $[(HPO_3)_2(P_2O_7)Mo_{30}O_{90}]^{8-}$ anion was the first example of POMs being electrochemically reduced by two electrons in neutral media. The presence of H^+ or Li^+ produced new two-electron waves at more positive potentials.

Experimental Section

Instrumentation. X-ray diffractions were measured at 193 K on a Bruker-AXS SMART 1000 diffractometer equipped with a CCD detector using graphite-monochromated Mo Kα radiation (0.71073 Å). The crystal structure was solved by direct method, and refined by full-matrix least-squares calculations based on F_o^2 using a program package SHELX97.[14] A Bruker Model AVANCE 500 spectrometer was used to record ^{31}P NMR spectra using a 5 mm diameter NMR tube with a concentric capillary containing D_2O for instrumental lock. Chemical shifts are expressed in parts per million with respect to 85% (v/v) H_3PO_4. Cyclic voltammograms were recorded with a HUSO Model HECS-311C potentiostat interfaced to a microcomputer-controlled system. A Tokai glassy carbon (GC-30S) with a diameter of 5.0 mm was used as a working electrode and a platinum wire served as the counter electrode. The voltage scan rate was set at 100 mV s^{-1}. The potentials are referred to the redox potential of ferrocene (Fc)/ferrocenium ion (Fc^+) as an internal reference. Prior to each measurement, the GC electrode was polished manually with 0.25 μm diamond slurry and washed with CH_3CN. The voltammetric measurements were made at 25 ± 0.1 °C. Coulometric analysis was made with a Hokuto Denko model HA-501 potentiostat equipped with a model HF-202D coulometer. A Thermo Nicolet model Avatar 360 spectrophotometer was used to record IR spectra as KBr pellets. UV−vis spectra were recorded on a Hitachi model U-3000 spectrophotometer.

Supporting Information Available: X-ray crystallographic data, Table S1 (interatomic distances concerning possible hydrogen bonding), Figure S1 (drawing concerning Pr_4N^+ cations in the crystal) and Figure S2 (UV−vis spectra). This material is available free of charge via the Internet at http://pubs.acs.org.

IC801499Y

(13) Himeno, S.; Sano, K.; Niiya, H.; Yamazaki, Y.; Ueda, T.; Hori, T. *Inorg. Chim. Acta* **1998**, *281*, 214.
(14) Sheldrick, G. M. *SHELX97*; University of Göttingen: Germany, 1997.